Covariance Matrix Estimation Errors and Diagonal Loading in Adaptive Arrays

BLAIR D. CARLSON, Member, IEEE
Lincoln Laboratory
M.I.T.

The use of adaptive beamforming techniques in which the radiation pattern of arrays of elements may be adaptively changed to reject interference signals, can provide significant performance advantages in radar, communication, and sonar applications. Simulations have been used to investigate the effect of covariance matrix sample size on the system performance of adaptive arrays using the sample matrix inversion (SMI) algorithm. Inadequate estimation of the covariance matrix results in adapted antenna patterns with high sidelobes and distorted mainbeams. A technique to reduce these effects by modifying the covariance matrix estimate is described from the point of view of eigenvector decomposition. This technique reduces the system nulling capability against low-level interference, but parametric studies show that it is an effective approach in many situations.

Manuscript received July 16, 1987; revised December 29, 1987.

This work was supported by the United States Department of the Navy under Electronic Systems Division Contract F19628-85-C-0002.

Author's address: Massachusetts Institute of Technology, Lincoln Laboratory, AN1-2H, P.O. Box 73, Lexington, MA 02173.

0018-9251/88/0700-0397 $1.00 © 1988 IEEE

I. INTRODUCTION

In adaptive array antennas using the sample matrix inversion (SMI) algorithm, the number of independent samples K used to generate the covariance matrix estimate affects the adapted beam gain and sidelobe structure. The estimated covariance matrix R is defined by

$$R = \frac{1}{K} \sum_{i=1}^{K} X_i X_i^{\dagger} \tag{1}$$

where X is a complex sample vector of receiver outputs of length N, N is the number of elements, K is the number of sample vectors used, and $\dagger$ denotes the transpose complex conjugate operation.

The array weights which produce the highest signal-to-interference-plus-noise ratio (Fig. 1) are given by [1]

$$W = R^{-1} V \tag{2}$$

where V is a steering vector of length N which is equal to the unadapted array weights.

Reed, Mallet, and Brennan [1] have shown that as K increases, the optimum signal-to-interference-plus-noise ratio performance is approached to within a factor ρ where the expected value of ρ is given by

$$E(\rho) = \frac{K + 2 - N}{K + 1}. \tag{3}$$

It can be seen that the expected value of the signal-to-interference ratio is within 3 dB of optimum when $K = 2N - 3$. The variance of ρ was shown by Boroson [2] to be

$$\mathrm{var}(\rho) = \frac{(K - N + 2)(N - 1)}{(K + 1)^2 (K + 2)}. \tag{4}$$

Other results given by Hudson [3] suggest that effective nulling can be achieved with K equal to twice the number of strong interference sources if N is much larger than the number of sources and only strong sources are present. This would suggest that in many applications, very few samples are needed for the covariance matrix. Gabriel [4], and Brookner and Howell [5] have shown, however, that while few samples are needed for effective interference suppression, the adaptive algorithm generates a pattern with distorted mainbeam and high sidelobes. Distorted beam shapes and high sidelobes may not be acceptable for reasons of clutter rejection, the need to avoid sidelobe target detection, and inaccuracy in target angle estimation. Kelly [6] has shown by extending Boroson's [2] results that the expected value of the pattern in the sidelobe region is equal to

$$E(SLL) = \frac{1}{K + 1}. \tag{5}$$

This indicates, for example, that in order to achieve -40 dB average sidelobes in the adapted pattern, 10,000 samples must be used in estimating R and the quiescent

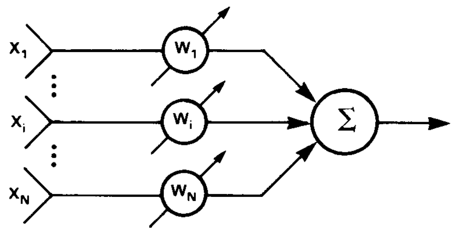

Fig. 1. Adaptive array beamformer.

(unadapted) beam shape must be below the -40 dB level.

Section II describes a computer simulation that was used to demonstrate these effects. Section III interprets these effects analytically from the point of view of eigenvector decomposition, and simulation results are presented. Section IV describes a way of alleviating these problems by diagonally loading the estimated covariance matrix. Results of simulations using this method are presented along with parametric studies which are useful in extending this analysis and method to other interference scenarios.

II. SIMULATION

The effects of covariance matrix sampling and estimation errors is evaluated with computer simulation techniques. A computer program was written which produced simulated spatially correlated and uncorrelated Gaussian noise for each of the channels in an adaptive array. The data streams were sampled and processed in an SMI algorithm. In all examples here, a 14-channel linear array ($\lambda/2$ spacing) is used. A Hamming weighted steering vector provided a quiescent beam with -41 dB sidelobes. The beam was steered to 20° from broadside. All of the elements have a cosine element pattern. A simulated interference source was placed at 0° with a power level 56 dB above the thermal noise level on the channels. Exact matching of the receiver channel transfer functions was assumed. Dispersion effects due to signal bandwidth also were incorporated in the simulation; however, these effects are not apparent in the results described due to the broadside location of the interference source. The effects of dispersion are discussed in Section IV.

Figs. 2 and 3 show adapted beam shapes where $2N$ and $6N$ samples are used, respectively. Virtually perfect nulling was achieved in both cases as well as in cases with as few as 4 samples, verifying Hudson's statement. Note that with fewer than N samples the matrix R is singular and cannot be inverted without augmenting or loading the matrix as defined in (6).

$$R_L = R + IL \tag{6}$$

where I is the identity matrix and L is a real constant representing a small load level. The average sidelobes in the patterns shown in Figs. 2 and 3 are at the

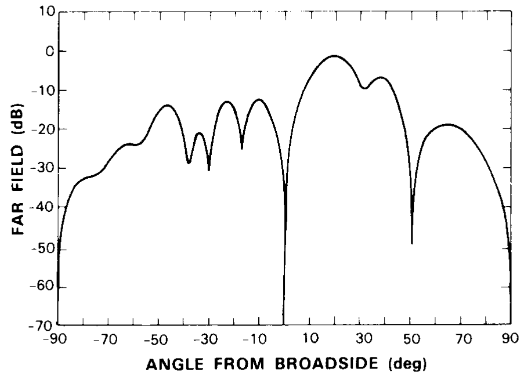

Fig. 2. Adapted beam shape with $2N$ samples. Jammer at 0° and steering vector at 20°.

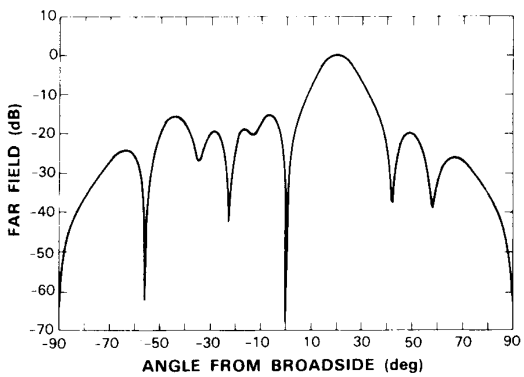

Fig. 3. Adapted beam shape with $6N$ samples. Jammer at 0° and steering vector at 20°.

approximate level predicted through the application of (5) (i.e., -14.5 dB and -19.2 dB, respectively). These levels of sidelobes and beam distortions may be unacceptably high for many applications even though the beam shape is optimum from a signal-to-interference-plus-noise point of view for a target in the exact direction of the steering vector.

III. EIGENVECTOR DECOMPOSITION

These effects can be interpreted and understood by considering the SMI optimum beam shape as a subtraction of eigenbeams from the quiescent pattern [4, 7].

$$G_v(\theta) = Q_v(\theta) - \sum_{i=1}^{N} \left(\frac{\lambda_i - \lambda_{\min}}{\lambda_i}\right) E_{iv}(\theta)(E_{iv}(\theta) \cdot Q_v(\theta)) \tag{7}$$

where $G_v(\theta)$ is the adapted beam pattern (voltage), $Q_v(\theta)$ is the quiescent beam pattern (voltage), λ_i is an eigenvalue of R, and $E_{iv}(\theta)$ is an eigenbeam of R (voltage). Eigenbeams are the beam shapes that are produced if the eigenvectors of R are used as weights in the array. Eigenvectors represent the modes of correlation in the R matrix and for a noise field consisting of strong uncorrelated plane wave interferences, the eigenbeams usually appear as beams pointed in the direction of the interference. The eigenvalues represent the energy associated with various correlation modes. Since the R matrix is Hermitian, all of the eigenvalues are real and the eigenbeams are orthogonal. The $(E_{iv}(\theta) \cdot Q_v(\theta))$ factor in (7) scales the eigenbeams to the proper size so that a null is produced in the directions of the interference when the eigenbeams are subtracted from the quiescent pattern. The $\frac{\lambda_i - \lambda_{\min}}{\lambda_i}$ factor in (7) approaches 1.0 for large eigenvalues associated with powerful interference sources and causes the eigenvalue energy to be nulled almost completely. For small eigenvalues near the noise level, this factor approaches 0.0 and no subtraction occurs. Since the dot product in (7) scales the interference eigenbeam to be equal to the quiescent beam in the interference direction, it is seen that the level of nulling below the quiescent beam shape for an interference source represented by a single eigenvalue is

$$\left(1 - \frac{\lambda_i - \lambda_{\min}}{\lambda_i}\right)^2 = \left(\frac{\lambda_{\min}}{\lambda_i}\right)^2. \tag{8}$$

This means that the quiescent pattern in the direction of the interference is reduced by twice the eigenvalue spread in dB.

Fig. 4 shows the eigenvalue structure of the estimated covariance matrix for the cases of $2N$ samples and $6N$ samples from the previous section. In both cases there is a single large eigenvalue corresponding to the interference source at a level of fourteen times the interference to noise level per element (i.e., 56 + 11.5 = 67.5 dB). The difference between the two cases is in the spread of the eigenvalues which correspond to the random noise. With few samples there is inadequate estimation of the noise and a large noise eigenvalue spread occurs with corresponding randomly shaped noise eigenbeams. As more samples are used, the estimation improves and the eigenvalues converge on the expected value of the noise. The SMI algorithm effectively subtracts portions of these randomly shaped noise eigenbeams from the quiescent pattern which causes the adapted beam shape to be distorted. Noise eigenbeam subtraction does not improve the signal-to-interference-plus-noise ratio when the adapted beam is used on a subsequent data set because the apparent noise correlations are different. Fig. 5 illustrates the spread of the noise eigenvalues (i.e., the ratio of the largest noise eigenvalue to the smallest, expressed in dB) as a function of the number of samples in the simulations. The convergence rate of the noise eigenvalues is slow after a large initial improvement. Each point represents a single simulation run.

The direct effect that noise eigenvalue spread has on the adapted beam shape can be seen in Figs. 6 and 7. Fig. 6 is a plot of the level of the highest sidelobe in the adapated beam shapes of the simulations as a function of the number of samples included in the covariance matrix estimate. Since the plot is of peak sidelobes, it is somewhat higher than the average sidelobes predicted by (5), however, they both have the characteristic of slow convergence. Fig. 7 shows the reduction of the gain in the adapted beam relative to the steady state adapted beam gain as a function of the number of samples used in the covariance matrix. Although nulling of the jammer signal is effectively accomplished even for small sample

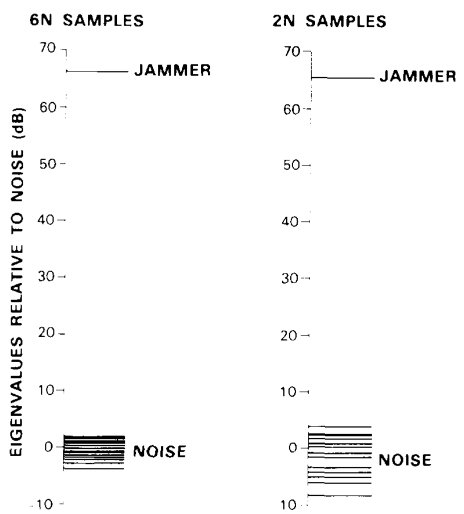

Fig. 4. Comparison of noise eigenvalues for $6N$ and $2N$ samples.

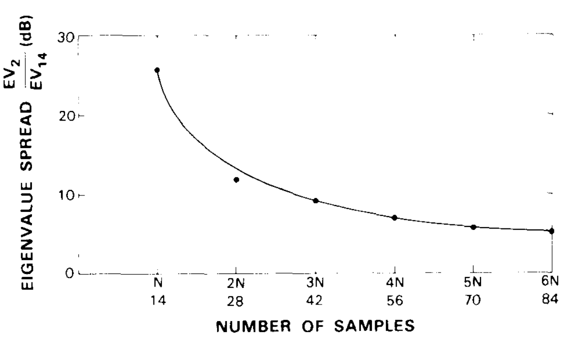

Fig. 5. Noise eigenvalue spread (ratio of largest noise eigenvalue to smallest) as function of number of independent samples included in covariance matrix.

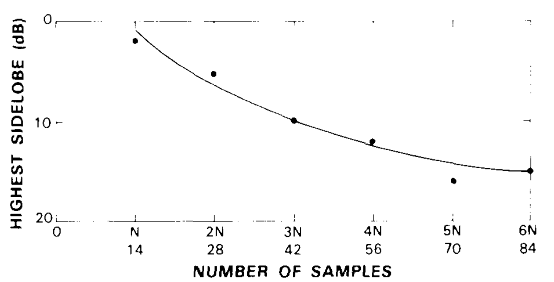

Fig. 6. Highest sidelobe in adapated patterns as function of number of independent samples included in covariance matrix. Hamming quiescent beam.

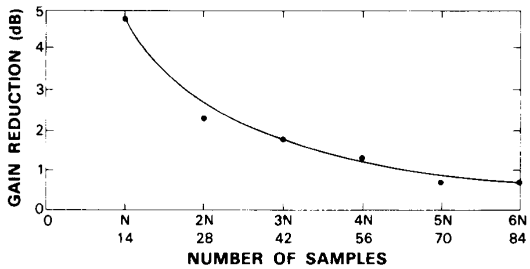

Fig. 7. Antenna gain reduction in adapted main beam as a function of number of independent samples included in covariance matrix.

sizes, the adapted beam gain reduction results in lower output signal power. Fig. 7 is a close match with (3) and the array gain reduction is a manifestation of the S/N performance factor given by Reed, Mallet, and Brennan (see (3)).

Avoiding the pattern degradation associated with the noise eigenvalue spread is essential in applications where the maximum antenna gain is required. The beam shape and sidelobe behavior are important for considerations such as avoiding clutter and sidelobe target returns, target angle estimation, and assuring that the adapted beam provides adequate regional coverage and not just optimum performance in the steered direction.

IV. DIAGONAL LOADING

If the noise eigenvalue spread is minimized, then the effects of randomly shaped noise eigenbeams is reduced and the adapted beam shape approaches the ideal pattern. Gabriel [4] has suggested that the covariance matrix modification, or loading, given in (6) can be used to accomplish this desired result. The eigenvalues of the loaded matrix are individually increased by the addition of L which is equivalent to increasing the covariance matrix diagonal by L. Large interference eigenvalues are minimally affected, but eigenvalues well below the load level are increased and compressed at the level L. The eigenvectors remain unchanged by diagonal loading. Fig. 8 shows an adapted beam shape for a simulation

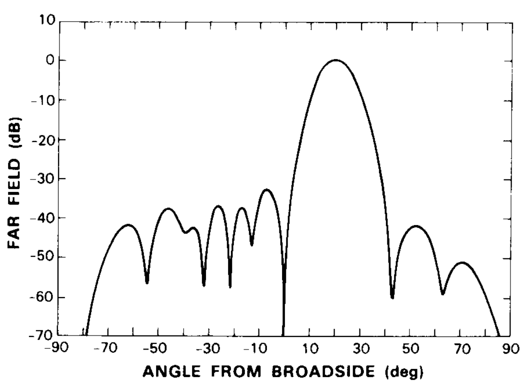

Fig. 8. Adapted beam shape with $6N$ samples and diagonal loading of 12 dB above noise level. Jammer at 0° and steering vector at 20°.

with $6N$ samples and loading with L at a level of 12 dB above the expected noise level. This example is identical to the conditions in Fig. 3 with the exception of loading. The principal interference source at 0.0 deg is effectively nulled in both cases, but the beam shape and sidelobes are significantly improved when diagonal loading is used.

Fig. 9 presents the resulting noise eigenvalue spread after diagonal loading as a function of loading level relative to thermal noise for simulations with several sample sizes. The physical implications of this can be seen in Figs. 10 and 11, which present the array sidelobe and gain behavior with respect to loading level.

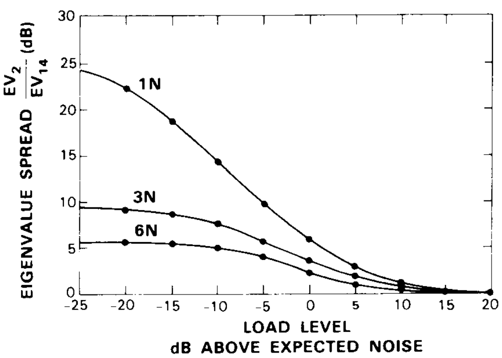

Fig. 9. Noise eigenvalue spread (ratio of largest noise eigenvalue to smallest) as function of loading level for $1N$, $3N$, and $6N$ independent samples in covariance matrix.

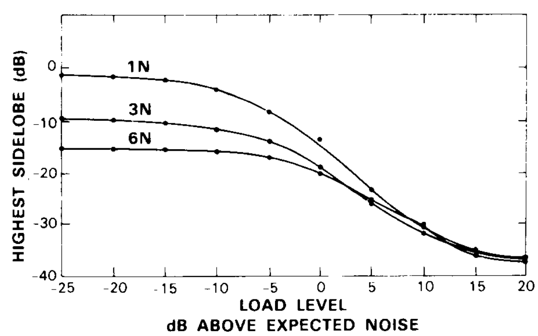

Fig. 10. Highest sidelobes in adapted pattern as function of loading level for $1N$, $3N$, and $6N$ independent samples in covariance matrix. Hamming quiescent beam.

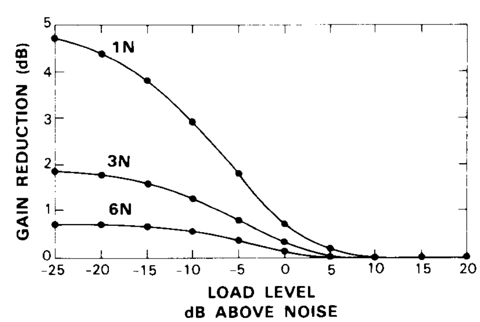

Fig. 11. Antenna gain reduction in adapted main beam as function of loading level for $1N$, $2N$, and $6N$ samples in covariance matrix.

Loading the diagonal as in (6) to compress the noise eigenvalues is equivalent to desensitizing the system by reducing the adaptive capability against small interference sources. When the elements are at half-wavelength spacing, adding the diagonal matrix to the true covariance matrix can be thought of as adding many small false jammers with all possible angles of arrival to the R matrix for purposes of antenna weight computation. While this desensitizing has almost no effect on nulling of interference represented by large eigenvalues, as can be seen from (8), it may reduce the system nulling capability against weak interference with small eigenvalues such as that which results from small jammers, residual energy from big jammers close in angle, residual jammer energy from dispersive effects.

When dispersive effects due to system bandwidth and time delays are present, a single interference source may have more than one eigenvalue associated with it. A principle eigenvalue contains most of the interference energy and one or more secondary eigenvalues contains the residual energy which decorrelates during the time delay. If these secondary eigenvalues are near the loading level, the nulling of the associated energy is reduced as can be seen from (8). A similar effect occurs when several jammers are close in angle to each other. Most of the combined energy is represented by a single eigenvalue, but due to small differences in the angles of arrival, a single correlation mode cannot represent all of the incident energy and secondary eigenvalues occur. When small interference eigenvalues are near the loading level and reduced nulling occurs as per (8), residual interference energy may remain after adapting. This remaining interference energy may be at an acceptable level because the source is weak by definition and the sidelobes of the adapted pattern provide further attenuation if the interference is spatially separated from the steering direction. There are many tradeoffs to consider when using this technique and while improving performance in many applications, excessive loading could result in unacceptable performance such as residual interference in others. It is apparent, however, from Figs. 10 and 11 that low loading levels can improve many aspects of performance, especially when the number of samples in the covariance estimate is small.

V. CONCLUSION

Inadequate estimation of the covariance matrix has a strong effect on system performance. Many of the problems associated with inadequate estimation can be ameliorated by diagonal loading. While this does have a desensitizing effect, it is an effective technique for many applications.

ACKNOWLEDGMENTS

I wish to thank T.P. Wallace of Lincoln Laboratory for the use of the data simulation program which he developed. I would also like to extend my thanks and appreciation to R.W. Katcher of Lincoln Laboratory for his programming assistance.

[1] Reed, I.S., Mallett, J.D., and Brennan, L.E. (1974)
Rapid convergence rate in adaptive antennas.
IEEE Transactions on Aerospace and Electronic Systems, AES 10, 6 (Nov. 1974).

[2] Boroson, D.M. (1980)
Sample size considerations for adaptive arrays.
IEEE Transactions on Aerospace and Electronics Systems, AES 16, 4 (July 1980).

[3] Hudson, J.E. (1981)
Adaptive Array Principles.
New York: Pereginus Ltd., 1981, p. 123.

[4] Gabriel, W.R. (1985)
Using spectral estimation techniques in adaptive array systems.
In *Proceedings of the Phase Arrays 1985 Symposium*, p. 109; also in-house report, RADC-TR-85-171, Rome Air Development Center, Griffiss Air Force Base, Rome, N.Y., Aug. 1985.

[5] Brookner, E., and Howell, J.M. (1985)
Adaptive-adaptive array processing.
In *Proceedings of the Phased Arrays 1985 Symposium*, p. 133; also in-house report, RADC-TR-85-171, Rome Air Development Center, Griffiss Air Force Base, Rome, N.Y., Aug. 1985.

[6] Kelly, E.J. (1987)
Adaptive detection in non-stationary interference, Part III. Technical Report 761, M.I.T. Lincoln Laboratory, Aug. 1987.

[7] Monzingo, R.A., and Miller, T.W. (1980)
Introduction to Adaptive Arrays.
New York: Wiley, 1980, p. 263.

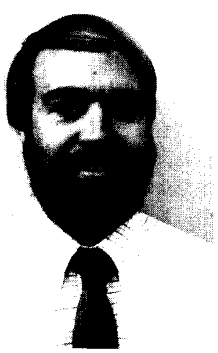

Blair D. Carlson (M'87) was born in Sewickley, Penn., on September 27, 1954. He received a B.S. degree in engineering science in 1976 from Pennsylvania State University, State College, PA and an M.E. degree in electrical engineering in 1978 from the University of Virginia, Charlottesville, VA.

He has worked in the areas of controls and dynamic systems. Since 1982 he has been employed at M.I.T. Lincoln Laboratory as a staff member involved in radar and antenna systems.